



Original Article

The impact of platelet rich fibrin on bone regeneration in critical-sized calvarial defects of rat model: A micro-computed tomographic analysis

Rayan Bakur Alkurdi, BDS¹, Ali Awad Alrahlah, PhD², Montaser Nazmi Alqutub, PhD¹

Departments of ¹Periodontics and Community Dentistry and ²Restorative Dental Sciences, King Saud University, Riyadh, Saudi Arabia.

***Corresponding author:**

Rayan Bakur Alkurdi,
Department of Periodontics
and Community Dentistry,
King Saud University, Riyadh,
Saudi Arabia.

rayanbalkurdi@gmail.com

Received: 08 October 2025
Accepted: 09 January 2026
Published: 01 March 2026

DOI
10.25259/IJHS_286_2025

Quick Response Code:



ABSTRACT

Objectives: Tooth loss can lead to alveolar bone resorption, complicating implant placement and requiring bone augmentation. While guided bone regeneration using autogenous or xenogenic grafts is standard, limitations such as donor site morbidity and variable outcomes persist. Platelet-rich fibrin (PRF), an autologous, growth factor-rich biomaterial, may enhance bone regeneration. To the best of our knowledge, this study provides a comparative evaluation of PRF combined with autograft, xenograft, and mixed grafts within the same critical-sized defect on a rat model (CSDs) using comprehensive micro-computed tomography (μ CT) analysis, providing a novel, standardized assessment of PRF's effects on bone regeneration.

Methods: Seventy male Wistar rats were randomly assigned to seven groups: negative control, bovine xenograft, autograft, mixed autograft + xenograft, and each of these combined with PRF. Standardized 5 mm CSDs were created and treated accordingly. PRF was prepared from autologous blood and applied with grafts when applicable. After 12 weeks, calvarial samples were analyzed using μ CT to assess new tissue and bone volume, percentage bone volume, trabecular structure, porosity, surface density, and bone mineral density (BMD). Data were analyzed using the Kruskal-Wallis nonparametric test with pairwise comparisons ($\alpha \leq 0.05$).

Results: All groups showed new bone formation. PRF-treated groups significantly outperformed graft-only groups. The PRF + autograft group showed the highest bone volume ($12.976 \pm 2.179 \text{ mm}^3$), trabecular thickness ($0.575 \pm 0.045 \text{ mm}$), and BMD ($0.541 \pm 0.061 \text{ g/cm}^3$) ($P < 0.001$), reflecting enhanced bone microarchitecture and mineral density based on μ CT analysis, with parameters trending toward those observed in native calvarial bone. The PRF + mixed graft group demonstrated superior percentage bone volume ($46.514 \pm 8.347\%$) compared to graft-only groups. The PRF + xenograft group similarly enhanced bone formation relative to graft-only controls; however, its regenerative effect remained lower than that achieved with PRF + autograft. PRF-treated defects exhibited more plate-like trabeculae and reduced trabecular separation.

Conclusion: Within the limitations of an animal model and a 12-week follow-up, PRF significantly enhanced bone regeneration based on quantitative μ CT parameters, particularly when combined with autograft. These findings provide experimental imaging evidence supporting the potential translational relevance of PRF, while highlighting the need for further biomechanical and clinical investigations.

Keywords: Bone graft, Critical-sized defect, Platelets-rich fibrin, Regeneration

How to cite this article: Alkurdi RB, Alrahlah AA, Alqutub MN. The impact of platelet rich fibrin on bone regeneration in critical-sized calvarial defects of rat model: A micro-computed tomographic analysis. Int J Health Sci (Qassim). 2026;20:85-97. doi: 10.25259/IJHS_286_2025

INTRODUCTION

Tooth loss, commonly resulting from dental caries or periodontal disease, leads to significant changes in the alveolar ridge that can compromise future implant placement.^[1,2] Alveolar bone resorption, particularly after tooth extraction, can reduce ridge volume by up to 30%.^[3] To address this, guided bone regeneration (GBR) is frequently used to promote new bone growth in deficient areas.^[4] Systematic reviews show high implant success rates, often above 90%, when ridge augmentation is performed.^[5] Autografts remain the gold standard due to their osteogenic and osseointegrative properties,^[6] but drawbacks such as donor site morbidity and limited availability encourage the use of alternatives such as allografts, xenografts, and alloplasts.^[7,8]

Effective GBR follows the PASS principles: primary closure, angiogenesis, space maintenance, and stability.^[9] Bone regeneration also relies on osseous cells, scaffolds, and bioactive materials. Adjunctive therapies, including curcumin, hyaluronic acid, and platelet concentrates, are used to enhance bone regeneration by leveraging growth factors such as bone morphogenetic proteins, platelet-derived growth factor (PDGF), transforming growth factor-beta (TGF- β), and vascular endothelial growth factor (VEGF).^[10] Given the inherent limitations of GBR, particularly dependence on passive scaffolds and delayed neovascularization, highlights the need for biologically active materials such as platelet-rich fibrin (PRF) that provide growth factors and a fibrin matrix to actively support bone regeneration. Platelet-rich plasma and PRF are two bioactive substances rich in growth factors that promote tissue healing and bone regeneration.^[11,12] PRF, a third-generation platelet concentrate developed by Choukroun, is prepared from the patient's blood without anticoagulants.^[13] During centrifugation, platelets and growth factors concentrate in a fibrin clot, which can be used alone or combined with other materials.^[14] PRF contains growth factors such as PDGF, TGF- β , and VEGF, which stimulate bone and soft tissue regeneration.^[15] It has been used successfully in periodontal therapy as a filling material or in combination with bone grafts to promote new bone formation.^[16,17]

Variants such as leukocyte-PRF can act as membranes or be mixed with bone grafts to create "sticky bone," improving handling and regenerative potential.^[18] As an autologous material, PRF is safe and carries minimal risk of immune reactions.

To the best of our knowledge, despite widespread clinical use of PRF, its comparative effects across multiple graft types have not been extensively investigated within a unified experimental model; thus, this micro-computed tomography (μ CT)-based evaluation of PRF with autograft, xenograft, and mixed grafts provides a comparative experimental

assessment that has not been extensively investigated and offers novel insights with potential translational relevance. This study aims to evaluate, *in vivo*, the regenerative effect of PRF on bone formation in critical-size defects (CSDs) in rats using μ CT, with the goal of improving experimental understanding of bone regeneration mechanisms relevant to alveolar bone regeneration.

MATERIALS & METHODS

Research ethical approval

Ethical approval was granted by the Institutional Review Board at King Saud University, reference number: KSU-SE-24-61, and the Ethics Committee, College of Dentistry Research Center (CDRC) at King Saud University, reference number: PR-0186. The study was done in compliance with the recommendations of the Animal Research: Reporting of *In vivo* Experiments.^[19]

Study design and sample size calculation

The study followed a double-blinded, randomized, controlled *in vivo* design. The sample size was determined by G Power software, with an alpha of 0.05, a power level at 0.90, effect size $f = 0.4$, and an attrition rate of 20%.

Experimental animal preparation

Seventy healthy male *Rattus norvegicus*, Albinus, Wistar rats, aged 3–4 months, weighing 250–300 g, were selected. The rats were housed in an experimental animal room with 50% humidity and 22°C. They were kept in individual metabolic cages with a light cycle of 12 h (6 AM–6 PM) 1 week before the start of the experiment to get acclimated to the environment and fed a standard laboratory diet and water.^[20-22]

Throughout the experiment, the specimens were placed under veterinary care. Due to the nature of the experiment being a surgical intervention, the rats were expected to be subjected to surgery-related risks, including bleeding, infection, swelling, or stress. An assigned professional veterinary doctor was present, monitoring the specimen throughout the experiment once daily, noting any adverse effects that might follow the surgery. In case the specimen showed signs of infection, pain, or discomfort, topical analgesia or antibiotics were administered.^[23]

Animal grouping, allocation, randomization, and blinding

The samples were randomly assigned to one of the seven experimental groups by simple randomization method using sequence generation (computer-based using www.randomizer.org), which are:

- (1) No treatment ($n = 10$), negative controls
- (2) Using bovine bone grafts ($n = 10$), positive controls.
- (3) Using PRF with bovine bone grafts ($n = 10$).
- (4) Using autogenous bone grafts ($n = 10$), positive controls.
- (5) Using PRF with autogenous bone grafts ($n = 10$)
- (6) Using a mixture of autogenous and bovine bone grafts ($n = 10$), positive controls.
- (7) Using PRF with a mixture of autogenous and bovine bone grafts ($n = 10$).

The sample was monitored throughout the experiment over 12 weeks before euthanasia. After euthanasia, A single investigator performed sample collection while being blinded to which grafting method was conducted during the surgery [Figure 1].

PRF preparation

Following an established injectable PRF (i-PRF) protocol, both PRF and sticky bone were prepared.^[24] Although direct biochemical quantification of growth factor concentration was not performed in this study, the PRF was produced using a standard low-speed centrifugation procedure, which has been extensively applied in previous work. This protocol produces PRF in a fibrin matrix structure and consistent flow of platelets and leukocytes and maintains a constant release of the PDGF, TGF- and VEGF over a 7–14-day period, allowing for predictable and sustained release of important growth factors such as PDGF, TGF-, and VEGF. Thus, the morphological and biological integrity of PRF employed in this experiment is reliant on the adherence to the low-speed centrifugation concept, which has been shown to enhance growth factor release, cellular migration, and biocompatibility.^[24] A blood sample was collected from the tail vein. The rat's tail is first warmed with a heat lamp to dilate the veins, and a small incision is made to collect the blood. This method is used for collecting small amounts of blood and is suitable for tests that require minimal manipulation of the blood sample.^[25] For male *Rattus norvegicus*, *Albinus*,

Wistar rats, the total amount should not exceed 10% of their total blood volume. For rats weighing 250–300 g, a total of 1.5–2 mL blood was collected per tube.^[26] For sticky bone preparation, the blood withdrawal time was around 15 s for each specimen, collected into one 10 mL tube (S-PRF tube; Avtec medical, Mt Pleasant, SC, USA) and immediately centrifuged at 1300 RPM for 14 min at a fixed centrifugation angle of 45° using Dr. Choukroun Duo Quattro PRF Centrifuge (Process for PRF, Rue Gioffredo, Nice, France). Following centrifugation, the blood sample was separated into three components in each vial: Red blood cells; a fibrin rich region, representing PRF; and acellular plasma. Liquid PRF was retrieved by directly separating it from the tube using a 2 mL syringe.^[27] Then, depending on the allocated group, it was mixed in a 1:1 ratio with either autogenous or xenogenic bony particles or both.

Pharmacological protocols

According to the pharmacological protocol of the Experimental Surgery and Animal Laboratory at King Khalid University Hospital, all surgical procedures were done under general anesthesia (50% ketamine: 5 mg/kg with 2% xylazine: 2 mg/kg xylazine - IV) with local anesthesia (2% lidocaine with 1:80,000 epinephrine) at the planned sites. Enrofloxacin (25 mg/kg - IM) prophylactic antibiotic was given prior to any surgical procedure. Flunixin (2 mg/kg - IV) was administered as an anti-inflammatory and analgesic for 3 days.

Important parameters such as respiratory rate, mucous membrane color, reflex response, and cellular tone were monitored by the attending veterinarian staff at all surgeries to maintain physiological stability. The pedal withdrawal reflex, palpebral reflex, and response to noxious stimuli were tested before and during the surgery and regularly throughout the surgery. If any light anesthesia was detected, then a second intraperitoneal anesthetic was administered. This process followed with four procedures in which animals

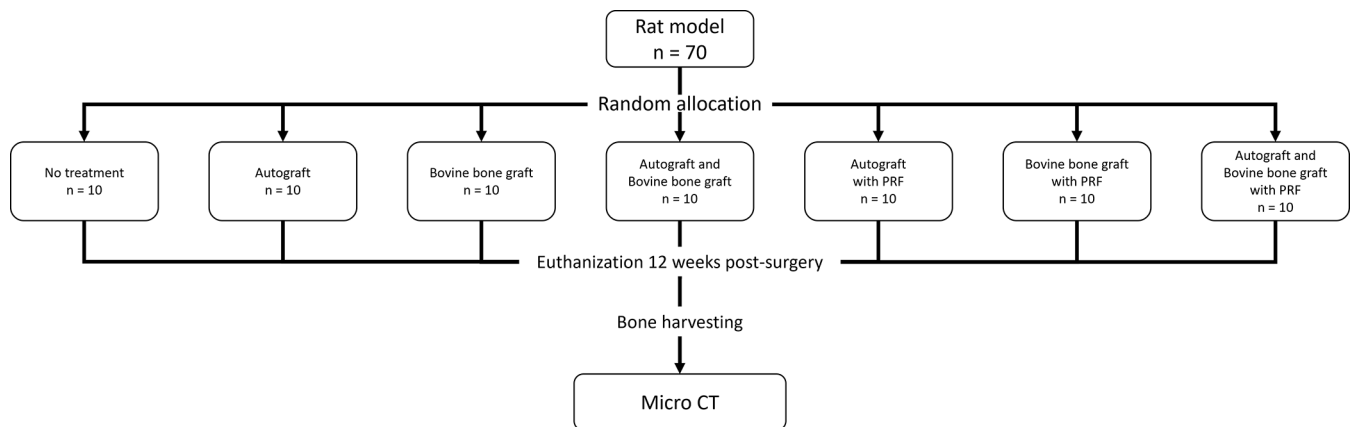


Figure 1: Flowchart of study design and sample distribution.

were monitored on hot recovery in a heated recovery chamber until they recovered spontaneous movement, normal respiration, and righting reflex. However, the animal returned to the cages and would be monitored regularly for the first 24 h as if it was experiencing a postoperative infection, discomfort, or delay in recovery.^[28]

Surgical protocol

All procedures involved in the surgery were performed by the same experienced surgeon to ensure no inter-operative variation. The surgical variability was further minimized by standardizing the surgical protocol, using identical instruments and drill characteristics, and performing all procedures using identical flap design and defect creation technique. The surgeon also performed a calibration phase on pilot specimens for reproducibility of defect size, drilling depth, and flap handling before beginning the experimental phase. Before starting the surgery, the animal was positioned in the prone position, and the scalp was disinfected with a povidone-iodine solution and shaved. A straight cutaneous incision of 15 mm was made in the scalp's midline on the sagittal suture over the parietal bone. The skin, periosteum, and all underlying tissues were reflected bilaterally to fully expose the calvaria with a full-thickness flap to utilize the periosteum as a membrane.^[29] On the parietal region lateral to the sagittal suture, a standardized 5 mm critical-sized defect was created by a trephine drill (Straumann AG, Waldenburg, Switzerland). The 5 mm full-thickness calvarial defect has been widely established as a CSD in rats, as demonstrated in the literature, which showed that defects of this dimension

do not reliably heal spontaneously and therefore provide an appropriate non-healing model for evaluating bone regeneration strategies.^[30] The defect was created to a depth of 2 mm and an outer diameter of 5 mm using a low-speed handpiece 1500 rpm with continuous sterile saline irrigation with caution to not damage the dura during removing the full thickness of bone which included the outer and inner cortices [Figure 2]. Following that, the extracted bone was handed to a single experienced assistant and depending on the group, a different type of bone was prepared with or without PRF. Once the graft mix is ready, the assistant would then hand the prepared graft to the blinded surgeon to apply to the created defect. For the Autograft groups, autograft from the same specimen was crushed using Bone Mill Forceps (Helmut Zepf Dental Instruments, Obere Hauptstraße 16-22 78606 Seitingen-Oberflacht, Germany) were added to the defect, for xenograft groups, bovine bone substitute was added to the defect (particle size: 0.25–1 mm, Bio-Oss[®]; Geistlich Pharma AG) And for mixed graft groups a ratio of 1:1 crushed autograft to xenograft was added to the defect. The same surgical protocol was followed in the PRF groups with the addition of PRF to the bone and adapting the mix into the defect. The surgical site was closed using Vicryl 5-0, 13 mm, 3/8 circle, absorbable violet braided suture (Ethicon, Inc., Johnson and Johnson, Raritan, New Jersey, United States), using a simple continuous suture technique [Figure 3].

Euthanasia

After 12 weeks of the study experiment, all rats were sacrificed using Carbon dioxide (CO₂) gas. The animals'

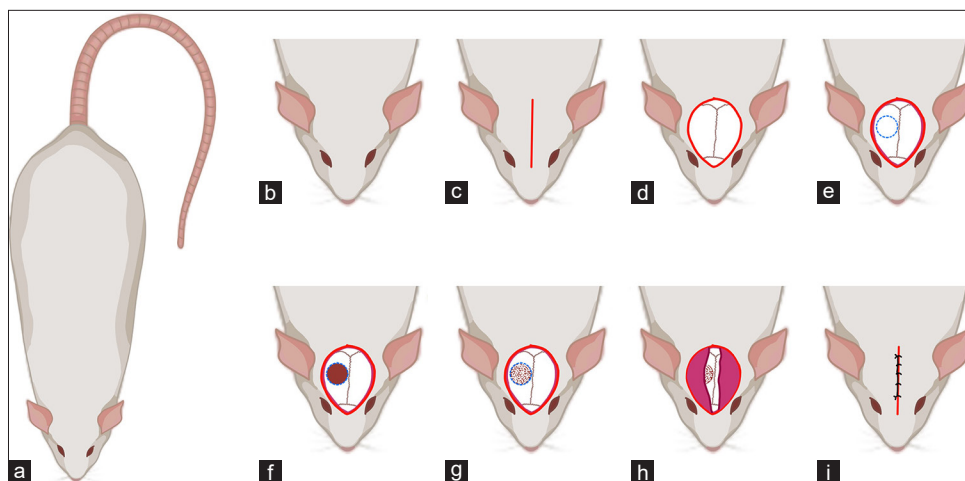


Figure 2: Illustration of the standardized calvarial defect. (a) After administering anesthesia and preparing the specimen for the surgery. (b) The rat's head is shaved in preparation for disinfection and incision. (c) A 15-mm midline incision was made along the sagittal suture over the parietal bone. (d) The skin, periosteum, and underlying tissues were bilaterally reflected to expose the calvarial surface using a full-thickness flap. (e) Locating the drilling area on the left of the sagittal suture. (f) A standardized 5 mm diameter critical-sized defect was created in the parietal bone lateral to the sagittal suture using a trephine drill. (g) Different grafting materials were placed into the defect site. (h) Periosteum adaptation for suturing. (i) The site sutured, engaging both the skin and periosteum.

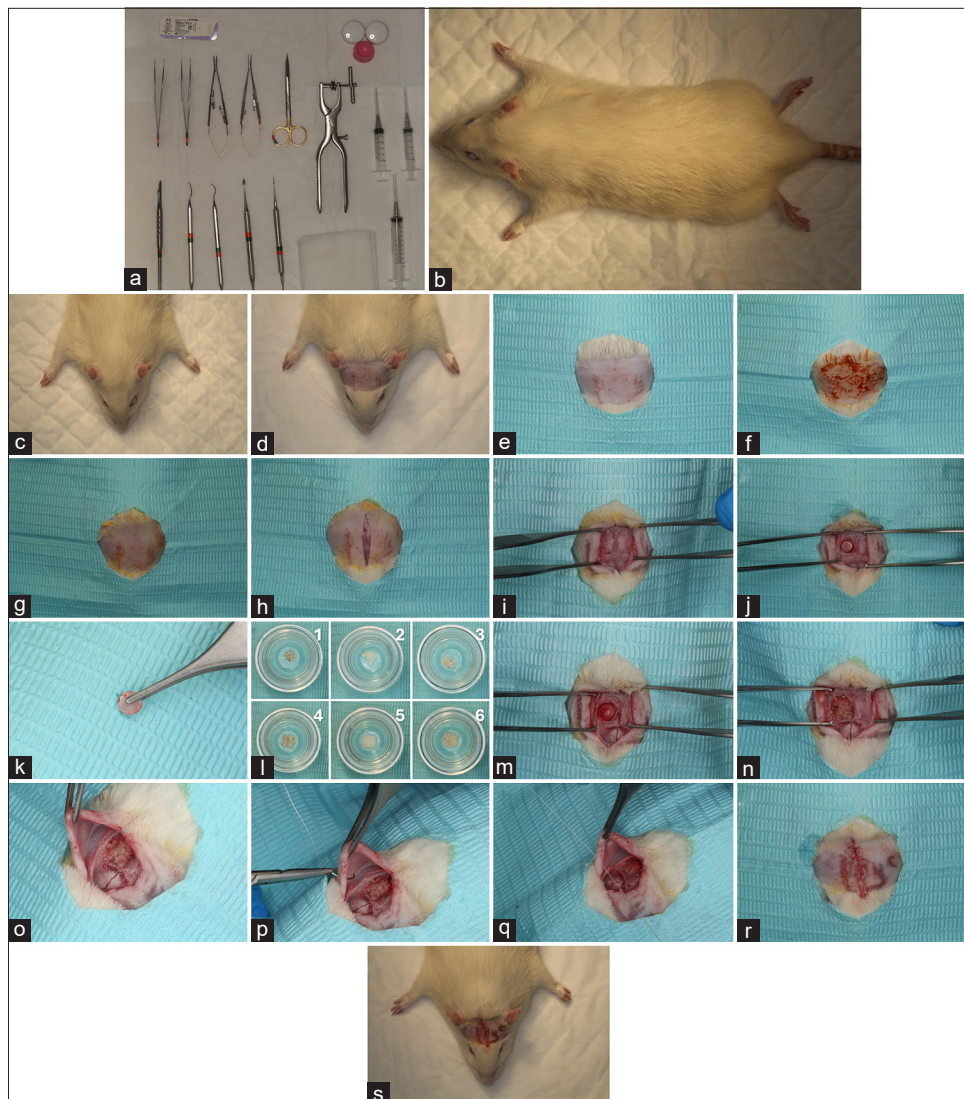


Figure 3: Photographs showcasing the surgical protocol. (a) Instrumentation. (b and c) After administering anesthesia and preparing the specimen for the surgery. (d and e) The rat's head is shaven in preparation for disinfection and incision. (f) Disinfected using a povidone-iodine solution. (g) Wiping the povidone-iodine solution away. (h) A 15-mm midline incision was made along the sagittal suture over the parietal bone. (i) The skin, periosteum, and underlying tissues were bilaterally reflected to expose the calvarial surface using a full-thickness flap and locating the drilling area on the left of the sagittal suture. (j) A standardized 5 mm diameter critical-sized defect was created in the parietal bone lateral to the sagittal suture using a trephine drill. (k) The calvarial bone was removed in preparation for grafting. (l) Bone graft preparation, (L-1) Autograft, (L-2) Xenograft, (L-3) Mixed autograft with xenograft, (L-4) platelet-rich fibrin (PRF) + Autograft, (L-5) PRF + Xenograft, (L-6) PRF + Mixed autograft with xenograft. (m) Grafting site irrigation. (n) Graft adaptation. (o) Locating and adapting the periosteum. (p) Suturing. (q) Engaging both the skin and periosteum. (r and s) Sutured using a continuous interlocked suture technique.

home cages were placed inside a CO₂ euthanasia chamber and continuously observed throughout the entire procedure, as shown in Figure 4. Using compressed CO₂ gas in cylinders as a source of CO₂ allows the inflow of gas to the

induction chamber to be controlled. Without pre-charging the chamber, 100% CO₂ was introduced at a fill rate of 30-70% displacement of the chamber volume per minute with CO₂, added to the existing air in the chamber. The expected

time to unconsciousness was within 2–3 min.^[31] The area of the surgical defect and the adjacent tissues were sectioned *en bloc*. 10% neutral formalin for 24 h was used for the fixation of the blocks.

Sample collection

A single investigator performed the sample collection while being blinded to the material used for each specimen. Using a round drill in a low-speed handpiece at 1500 rpm with continuous sterile saline irrigation, the area of the surgical defect was sectioned off with an outer margin of normal bone in Figure 5. The full thickness of bone was harvested for microcomputed tomography.

Radiographic analysis μ CT imaging analysis

The μ CT imaging and analysis was done by a single blinded operator. The characteristics of newly formed bone (NFB), including tissue volume, bone volume, percentage bone volume, trabecular thickness, trabecular number, trabecular separation, structure model index (SMI), bone porosity, bone surface density, and bone mineral density (BMD), were quantitatively assessed. To generate a three-dimensional image for each scanned specimen, a μ CT system (Skyscan 1172, Bruker, Belgium) was used. Each sample was individually secured for imaging using paraffin wax film and mounted inside a polyethylene plastic container. These mounted samples were then placed on the micro-stage within the high-resolution μ CT specimen chamber.

Image acquisition was performed with the following settings: 60 kV tube voltage, 165 μ A anode current, 2065 ms exposure time, 17.27 μ m pixel resolution, 0.5 mm aluminum filter, 0.4° rotation step across a 180° range, frame averaging of 4 to

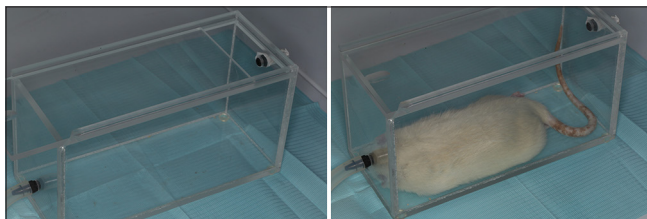


Figure 4: The CO₂ euthanasia chamber.



Figure 5: Sample collection of the area, including the surgical defect and an outer margin.

enhance signal-to-noise ratio, and random movement set to 8 to minimize ring artifacts. A flat-field correction was applied prior to scanning to address pixel sensitivity variations in the camera.

Following image capture, the projection data were reconstructed into cross-sectional slices using NRecon software (version 1.6.9.4; Bruker). Reconstruction parameters were carefully reviewed and adjusted to ensure optimal image quality. To avoid artificially increased density at the sample surface and reduced density in the center, beam hardening compensation was set to 25%, ring artifact reduction to 5, and image smoothing was applied using a Gaussian kernel with a value of 2. Final images were saved as 16-bit TIFF files.

These reconstructed images were imported into Data Viewer (version 1.5.6.2; Bruker) for quality evaluation, reorientation, resizing, and visual selection of regions of interest (ROI). A trans-axial dataset was then exported and analyzed using CTAn (version 1.17.7.2; Bruker), which provided tools for morphometric and densitometric analysis through surface rendering. CTAn was also employed to binarize and quantify NFB within the defect area.

To define the volume of interest, a manual freehand ROI was drawn to encompass only the NFB, excluding the surrounding natural bone. A threshold based on grayscale values was selected to isolate the relevant structures. Calibration of BMD measurements in g/cm^3 was achieved using a 4 mm diameter BMD phantom rod, representative of rat bone.

Finally, a 3D surface-rendered model was generated using a surface construction algorithm, and CTVol software (version 2.3.2.0; Bruker) was used for three-dimensional visualization of the samples.

Statistical analysis

The statistical analysis was conducted using the SPSS Statistics Software Package for Social Sciences (SPSS 28.0.1.1, IBM, NY, USA). Nonparametric tests were employed since the data followed a non-normal distribution using the Kolmogorov-Smirnov and Shapiro-Wilk tests. Variables are reported as mean \pm standard deviation (SD) to describe the quantitative and categorical variables. Group differences were assessed using the non-parametric Kruskal-Wallis test, with multiple comparisons carried out using the pairwise comparison test, considering a significance level of $\alpha \leq 0.05$.

RESULTS

μ CT findings

All μ CTs are reported in Table 1, with a comparison 3D rendering of a sample from each group showcased in Figure 6.

Table 1: Mean and SD* of the newly formed bone characteristics of the study groups.

Variable	Negative control	Mixed graft positive control	Xenograft positive control	Autograft positive control	PRF+Mixed graft	PRF+ Xenograft	PRF+ Autograft
Tissue volume	20.022±4.587	25.135±5.698	27.540±7.310	28.484±3.236	24.990±5.492	27.672±6.075	28.485±4.365
Bone volume	6.480±1.524	9.855±2.688	9.105±1.696	9.847±1.532	11.349±1.972	10.149±1.515	12.976±2.179
Percentage bone volume	32.625±5.167	38.901±2.040	35.262±11.489	34.779±5.358	46.514±8.347	37.601±6.300	45.528±3.509
Trabecular thickness	0.415±0.080	0.485±0.121	0.451±0.096	0.414±0.082	0.483±0.058	0.427±0.043	0.575±0.045
Trabecular number	0.746±0.139	0.825±0.068	0.820±0.337	0.853±0.167	1.025±0.086	1.051±0.159	1.060±0.214
Trabecular separation	0.566±0.157	0.517±0.087	0.635±0.350	0.587±0.139	0.447±0.084	0.493±0.054	0.508±0.048
Structure model index	2.136±0.821	2.157±0.727	1.855±0.742	0.858±0.658	1.523±1.349	1.635±1.048	1.557±1.056
Total volume of pore space	12.365±3.900	14.927±3.299	18.496±7.888	18.647±3.130	17.708±2.125	18.937±4.547	16.533±2.296
Bone surface density	3.292±0.756	3.545±0.312	3.121±1.182	3.037±0.671	3.563±0.289	3.561±0.215	3.145±0.352
Bone mineral density	0.327±0.046	0.445±0.034	0.391±0.128	0.413±0.057	0.522±0.078	0.466±0.076	0.541±0.061

*SD: Standard deviation, PRF: Platelet-rich fibrin

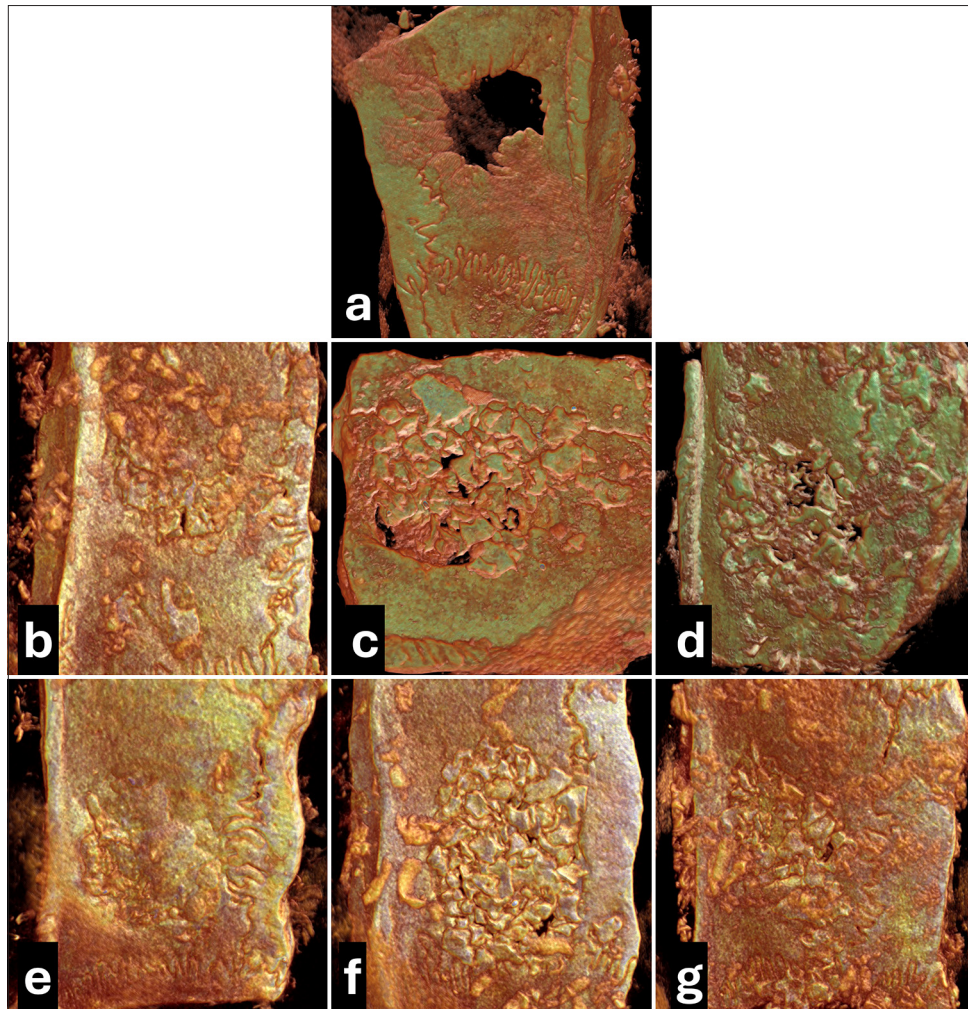


Figure 6: 3D rendering of micro-computed tomography images of the calvarial defects, new bone formation, and residual graft materials. (a) Negative control group. (b) Autograft positive control groups. (c) Xenograft positive control group. (d) Mixed graft positive control group. (e) Platelet-rich fibrin (PRF) + autograft group. (f) PRF + xenograft group. (g) PRF + mixed graft group.

Tissue volume

All groups demonstrated new tissue formation within the defect site. The PRF + autograft and the autograft positive control groups had the highest volumes ($28.485 \pm 4.365 \text{ mm}^3$ and $28.484 \pm 3.236 \text{ mm}^3$, respectively). These were followed by the PRF + xenograft and the xenograft positive control groups ($27.672 \pm 6.075 \text{ mm}^3$ and $27.540 \pm 7.310 \text{ mm}^3$), and the mixed graft positive control and the PRF + mixed graft groups ($25.135 \pm 5.698 \text{ mm}^3$ and $24.990 \pm 5.492 \text{ mm}^3$). The negative control group had the lowest volume ($20.022 \pm 4.587 \text{ mm}^3$), which was significantly lower than both the autograft positive control ($P < 0.001$) and the PRF + autograft groups ($P < 0.002$) [Graph 1].

Bone volume (new bone formation)

All study groups exhibited new bone formation within the defect sites. Among them, the PRF + autograft group showed the highest mean NFB volume ($12.976 \pm 2.179 \text{ mm}^3$), while the negative control group had the lowest ($6.480 \pm 1.524 \text{ mm}^3$). The other groups demonstrated intermediate NFB volumes: xenograft positive control ($9.105 \pm 1.696 \text{ mm}^3$), autograft positive control ($9.847 \pm 1.532 \text{ mm}^3$), mixed graft positive control ($9.855 \pm 2.688 \text{ mm}^3$), PRF + xenograft ($10.149 \pm$

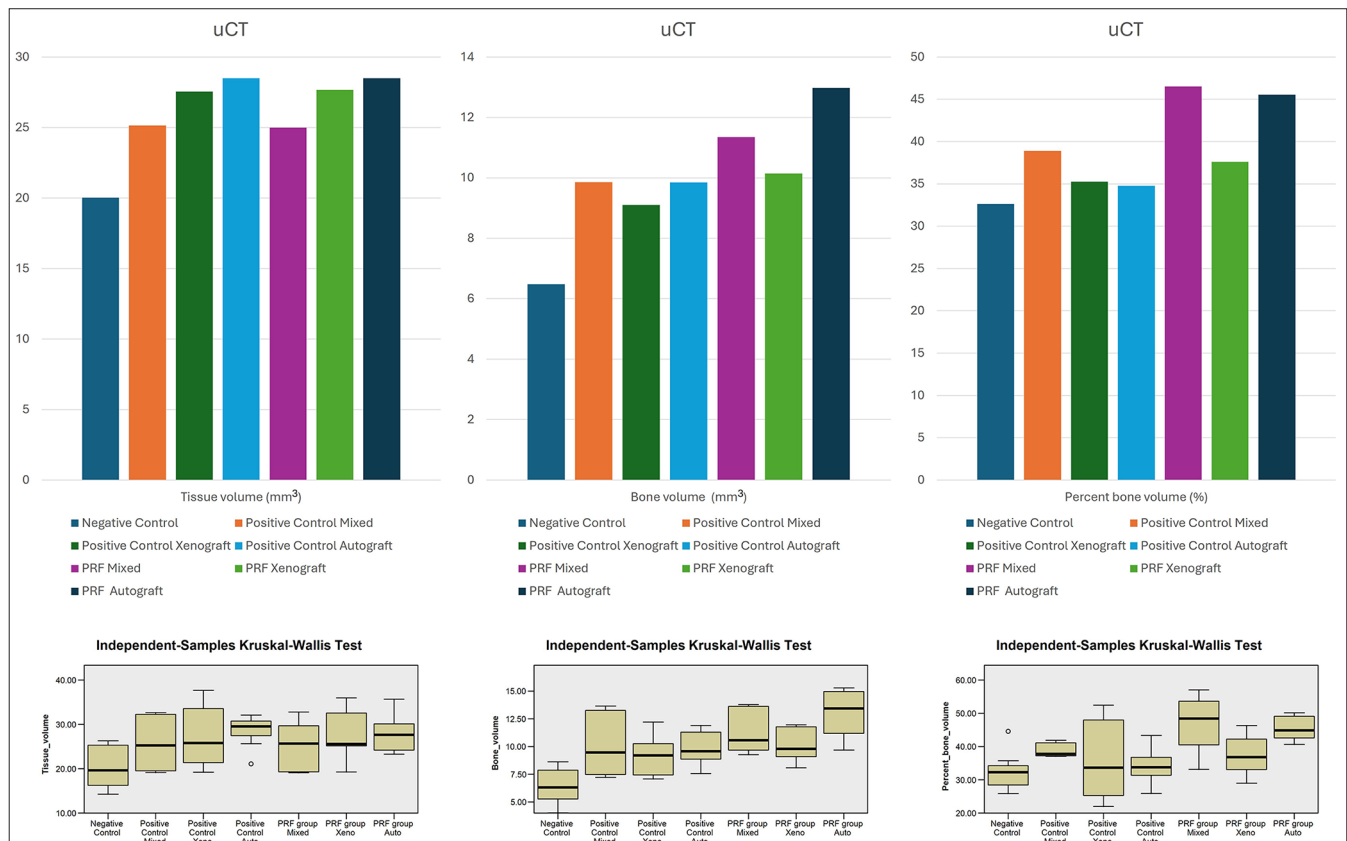
1.515 mm^3), and PRF + mixed graft ($11.349 \pm 1.972 \text{ mm}^3$). Statistically significant differences in NFB volume were observed between the negative control group and all PRF + bone graft groups, as well as between the xenograft positive control and the PRF + autograft group ($P < 0.001$) [Graph 1].

Percentage bone volume

The highest percentage of bone formation was observed in the PRF + mixed graft group ($46.514 \pm 8.347 \%$), followed closely by the PRF + autograft group ($45.528 \pm 3.509 \%$). In contrast, the negative control group exhibited the lowest bone formation percentage ($32.625 \pm 5.167 \%$). Statistically significant differences were found between the negative control group and both the PRF + autograft group and the PRF + mixed graft group ($P < 0.001$). In addition, a significant difference was noted between the xenograft positive control group and the PRF + autograft bone group ($P < 0.001$) [Graph 1].

Trabecular thickness

The greatest trabecular thickness was observed in the PRF + autograft group ($0.575 \pm 0.045 \text{ mm}$), whereas the lowest values were recorded in the autograft positive control (0.414



Graph 1: Comparing the newly formed bone characteristics of the study groups by tissue volume (mm^3), bone volume (mm^3), and percentage bone volume (%).

± 0.082 mm) and negative control (0.415 ± 0.080 mm) groups. Statistically significant differences in trabecular thickness were found between the PRF + autograft group and all the negative control group, the autograft positive control group, and the PRF + xenograft group ($P < 0.001$) [Graph 2].

Trabecular number

The lowest trabecular numbers were recorded in the negative control group (0.746 ± 0.139 1/mm) and the xenograft positive control group (0.820 ± 0.337 1/mm). In contrast, the highest trabecular number was observed in the PRF + autograft group (1.060 ± 0.214 1/mm), followed closely by the PRF + xenograft group (1.051 ± 0.159 1/mm). Statistically significant differences were found between the negative control group and all the PRF + autograft group, PRF + xenograft group, and PRF + mixed graft group ($P < 0.001$) [Graph 2].

Trabecular separation

Although not statistically significant, the xenograft positive control group exhibited the highest mean trabecular separation (0.635 ± 0.350 mm), followed by the autograft positive control (0.587 ± 0.139 mm) and the negative

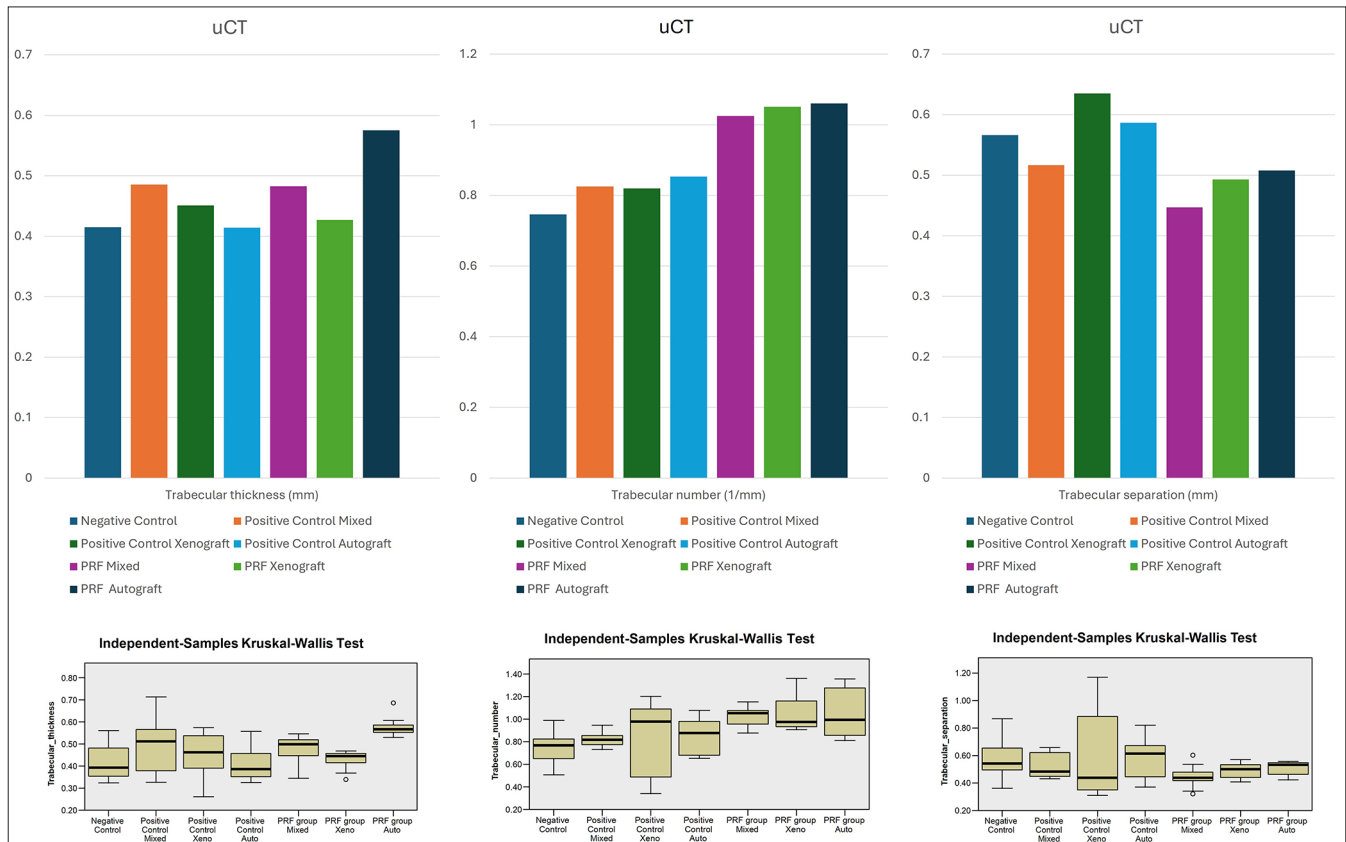
control group (0.566 ± 0.157 mm). In comparison, all PRF-treated groups showed lower trabecular separation, with the PRF + mixed graft group having the lowest value (0.447 ± 0.084 mm), followed by the PRF + xenograft (0.493 ± 0.054 mm) and PRF + autograft (0.508 ± 0.048 mm) groups [Graph 2].

SMI

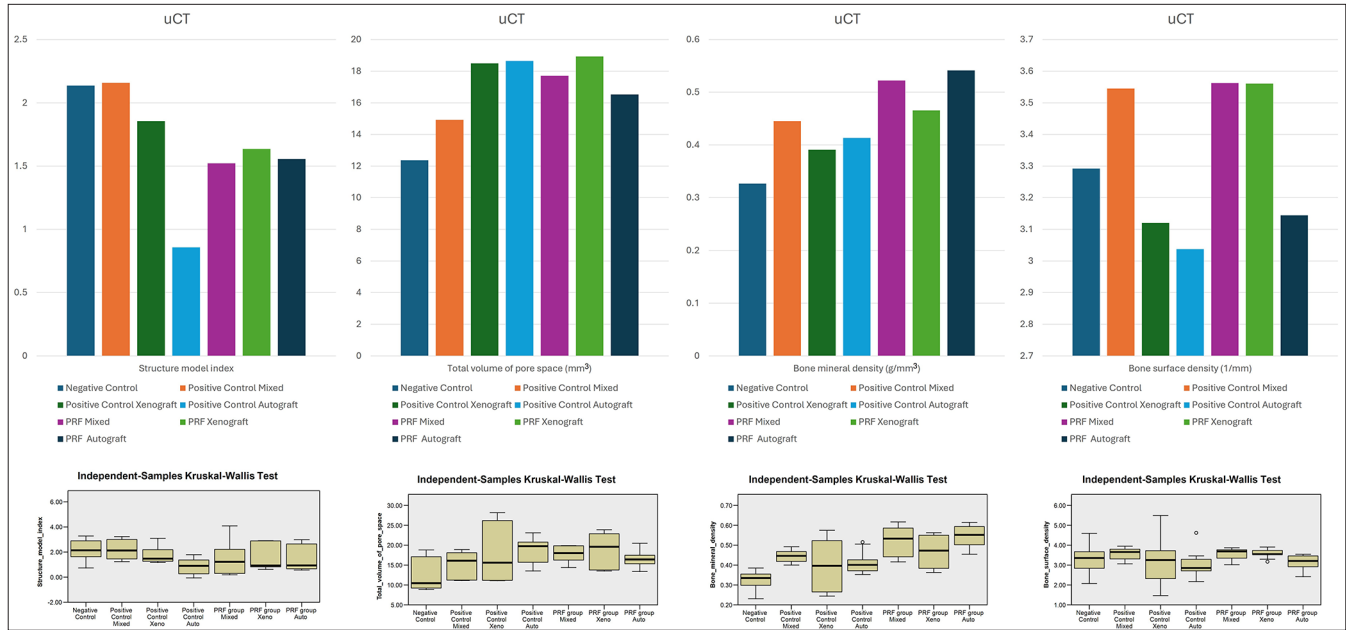
Analysis of the SMI revealed that the mixed graft positive control group (2.157 ± 0.727) and the negative control group (2.136 ± 0.821) exhibited values most consistent with a rod-like trabecular architecture. In contrast, the autograft positive control (0.858 ± 0.658) and the PRF + mixed graft group (1.523 ± 1.349) showed SMI values indicative of a more plate-like bone structure. A statistically significant difference was noted between the mixed graft positive control group and the autograft positive control group ($P < 0.002$) [Graph 3].

Total volume of pore space

The PRF + xenograft group exhibited the highest mean pore space volume (18.937 ± 4.547 mm³), followed closely by the autograft positive control (18.647 ± 3.1230 mm³) and the xenograft positive control groups (18.496 ± 7.888 mm³). In



Graph 2: Comparing the newly formed bone characteristics of the study groups by trabecular thickness (mm), trabecular number (1/mm), and trabecular separation (mm³).



Graph 3: Comparing the newly formed bone characteristics of the study groups by structure model index, total volume of pore space (mm³), bone surface density (1/mm), and bone mineral density (g/cm³).

contrast, the negative control group showed the lowest pore space volume (12.365 ± 3.900 mm³), which was statistically significantly lower compared to both the PRF + xenograft group ($P < 0.002$) and the autograft positive control group ($P < 0.001$) [Graph 3].

Bone surface density

While the differences were not statistically significant, the highest mean bone surface density was observed in the mixed graft positive control group (3.545 ± 0.312 1/mm), followed by the PRF + mixed graft group (3.563 ± 0.289 1/mm) and the PRF + xenograft group (3.561 ± 0.215 1/mm). In contrast, the lowest values were recorded in the autograft positive control group (3.037 ± 0.671 1/mm), followed by the xenograft positive control group (3.121 ± 1.182 1/mm) and the PRF + autograft group (3.145 ± 0.352 1/mm) [Graph 3].

BMD

The PRF + autograft group exhibited the highest mean BMD values (0.541 ± 0.061 g/cm³), followed by the PRF + mixed graft group (0.522 ± 0.078 g/cm³) and the PRF + xenograft group (0.466 ± 0.076 g/cm³). The lowest BMD was found in the negative control group (0.327 ± 0.046 g/cm³), showing statistically significant differences compared to all the PRF + autograft, PRF + mixed graft, and PRF + xenograft groups ($P < 0.001$). In addition, the PRF + autograft group demonstrated significantly higher BMD values than both the xenograft positive control ($P < 0.001$) and the autograft positive control ($P < 0.002$) groups [Graph 3].

DISCUSSION

This study evaluated the regenerative potential of PRF in critical-sized calvarial defects in rats, using μ CT to quantitatively analyze new bone formation and remodeling. The results demonstrated that PRF significantly enhanced bone regeneration when combined with grafting materials, particularly with autografts, compared to both negative controls and conventional grafting alone. The rat calvarial CSD model is a well-established and reliable *in vivo* system for evaluating novel bone regenerative materials and techniques. The 5 mm defect used in this study is widely accepted as appropriate for assessing new bone formation.^[32]

μ CT has become a standard, non-invasive three-dimensional imaging tool in experimental and preclinical research, capable of assessing both the quantity and quality of regenerating bone, often rivaling conventional histological techniques. The superior outcomes in the PRF + autograft group, reflected in significantly greater bone volume, trabecular thickness, and BMD, suggest that PRF plays a synergistic role in optimizing the osteogenic capacity of autogenous grafts. These findings are in line with previous reports that PRF, being a fibrin matrix enriched with platelets, leukocytes, and growth factors, supports angiogenesis, osteoblast proliferation, and sustained release of growth mediators, thereby accelerating early bone healing.^[24,26]

Interestingly, PRF also improved outcomes when combined with xenografts and mixed grafts. Groups treated with PRF + xenograft and PRF + mixed graft showed increased percentage bone volume, trabecular number, and BMD

compared with their respective controls. This suggests that PRF may compensate for the inherent limitations of xenogenic substitutes, which primarily serve as osteoconductive scaffolds but lack osteoinductive properties. The improved SMI values in PRF groups further indicate that PRF contributes to more plate-like, mechanically favorable trabecular architecture, which is essential for long-term stability.

The μ CT analysis also revealed reduced trabecular separation and higher BMD in PRF-treated groups. This indicates a more mature and denser trabecular network, which may be associated with structural features relevant to graft consolidation; however, clinical performance and biomechanical strength were not directly evaluated in this study. Of note, the PRF + autograft group not only showed significantly higher BMD compared to xenograft and autograft controls but also outperformed all other combinations, highlighting the biological advantage of autogenous bone as the gold standard grafting material.

However, despite these promising results, PRF did not entirely overcome the limitations of non-autogenous grafts. For example, pore space remained higher in PRF + xenograft groups compared with autografts, suggesting delayed graft resorption or incomplete replacement by native bone. This is consistent with the slow resorption profile of deproteinized bovine bone mineral such as Bio-Oss, which persists long-term within defects due to its high crystallinity and low turnover rate. Consequently, even when supplemented with PRF, xenografts may continue to act primarily as space-maintaining scaffolds rather than contributing substantially to new bone formation.^[33] These findings highlight the importance of graft selection and suggest that PRF acts as a potentiator rather than a substitute for bone-forming capacity.

Several studies have supported these data. An animal study showed that both PRF and GBR treatments resulted in similar increases in alveolar ridge volume and new bone formation based on μ CT analysis, suggesting that PRF is as effective as GBR for graft integration.^[34] PRF harvested on day 14 exhibited significantly greater peak mineralization compared to both the negative and positive control groups. This suggests that PRF may more effectively promote bone regeneration and hold promising potential for clinical applications.^[35] However, another study revealed no statistically significant difference in BMD between the PRF group, the PRF combined with freeze-dried bone allograft (FDBA) group, and the FDBA-alone group, with the negative control group showing significantly lower BMD.^[36] This discrepancy may be attributed to several key differences between the two studies. In their study, they evaluated ridge-preservation procedures in humans, a healing environment that inherently possesses osteogenic potential, which may

diminish the relative contribution of a biologically active adjunct such as PRF. In contrast, the present study employed a critically sized, non-healing calvarial defect in rats, a model in which the impact of PRF's angiogenic and regenerative properties is more readily observable. Furthermore, the graft material used in that study was FDBA, which exhibits a slow remodeling profile that may limit the degree to which PRF can enhance mineralization. In the current investigation, autografts, xenografts, and mixed grafts, each with distinct resorption dynamics, may have provided more compatible scaffolds for PRF-mediated early fibrin stabilization, cellular recruitment, and angiogenesis, thereby amplifying PRF's regenerative influence. These biological and material-based differences likely account for the contrasting BMD outcomes observed between the two studies.

Taken together, the collective improvements observed across bone volume, microarchitectural organization, and mineral density suggest that PRF does not merely accelerate early healing, but orchestrates a more coordinated and biologically mature form of bone regeneration. The concurrent increases in trabecular thickness and number, reduction in trabecular separation, and shift toward a plate-like architecture (lower SMI) indicate that PRF promotes the formation of a structurally efficient trabecular network optimized trabecular organization, which may be associated with improved structural competence; however, biomechanical performance was not directly evaluated in this study. When coupled with the significantly higher BMD, these microarchitectural changes imply that PRF enhances both the quantity and quality of regenerated bone. We propose that PRF exerts its effect by providing a sustained release of growth factors within a fibrin-rich scaffold that simultaneously supports angiogenesis, osteoblast recruitment, and mineral deposition, yielding bone that is more abundant and exhibits structural features indicative of advanced bone maturation based on μ CT-derived parameters. This hypothesis positions PRF, particularly in combination with autografts, as a biologically active catalyst capable of driving a more integrated and a regenerative process characterized by favorable microarchitectural organization and mineral density.

The translational significance of this study lies in its potential application for alveolar ridge augmentation and periodontal regenerative procedures. By enhancing graft integration and quality of regenerated bone, PRF could reduce morbidity, shorten healing times, and improve patient outcomes. Nonetheless, several limitations must be acknowledged. First, this was an animal model, and extrapolation to humans must be approached cautiously due to biological differences. Second, the observation period was limited to 12 weeks; longer-term studies are required to assess graft maturation and functional loading capacity. Third, histological evaluation, which could have provided insights into cellular

activity and vascularization, was not performed alongside μ CT.

Future research should focus on controlled clinical trials to validate these findings in humans, explore optimized PRF preparation protocols, and investigate synergistic use with emerging biomaterials or biologics.

CONCLUSION

Within the limitations of this study, PRF significantly enhanced bone regeneration in critical-sized calvarial defects in rats, particularly when combined with autogenous bone grafts. Among the tested groups, the PRF + autograft and PRF + mixed graft combinations emerged as the most effective in promoting osteogenesis, as evidenced by favorable μ CT outcomes. PRF improved bone volume, density, and trabecular architecture compared to grafting alone, underscoring its role as a biologically active adjunct that potentiates regenerative capacity within an experimental animal model. These findings support the potential translational relevance of PRF in bone regeneration, while emphasizing the need for biomechanical validation and clinical studies prior to clinical application, offering an experimentally supported strategy that warrants further evaluation in biomechanical testing and human clinical studies.

Acknowledgment: The authors would like to express their gratitude to the CDRC, King Saud University, Riyadh, Saudi Arabia, for its support throughout this study. Special thanks are extended to Engineer Abdullah Bugshan Research Chair for Dental and Oral Rehabilitation, College of Dentistry, King Saud University, Riyadh, Saudi Arabia, for their valuable assistance in using the μ CT device and software for image analysis and measurements.

Authors' contributions: Conceptualization, R.A. and M.A.; methodology, R.A. and M.A.; software, R.A.; validation, R.A. and M.A.; formal analysis, R.A.; investigation, R.A.; resources, R.A., M.A., and A.A.; data curation, R.A.; writing—original draft preparation, R.A. and M.A.; writing—review and editing, R.A. and M.A.; visualization, R.A. and M.A.; supervision, M.A.; Review and editing, R.A., M.A., and A.A.; All authors have read and agreed to the published version of the manuscript.

Ethical approval: The research/study was approved by the Institutional Review Board (IRB) at IRB, King Saud University, Medical City, number KSU-SE-24-61, dated October 21, 2024.

Declaration of patient consent: Patient's consent is not required as there are no patients in this study.

Financial support and sponsorship: Nil

Conflicts of interest: There are no conflicts of interest.

Availability of data and material: The datasets analyzed during the present study are available from the corresponding author upon reasonable request.

Use of Artificial Intelligence (AI)-Assisted Technology for manuscript preparation: Artificial intelligence (AI) tools were

used solely to assist with language editing. No AI tools were used for data extraction, statistical analysis, result interpretation, or the generation of original scientific content. All analyses were conducted by the authors, who take full responsibility for the integrity and accuracy of the manuscript.

REFERENCES

- Chisci G, Hatia A, Chisci E, Chisci D, Gennaro P, Gabriele G. Socket preservation after tooth extraction: Particulate autologous bone vs. Deproteinized bovine bone. *Bioengineering (Basel)* 2023;10:421.
- Haworth S, Shungin D, Kwak SY, Kim HY, West NX, Thomas SJ, *et al.* Tooth loss is a complex measure of oral disease: Determinants and methodological considerations. *Community Dent Oral Epidemiol* 2018;46:555-62.
- Tyrovolas S, Koyanagi A, Panagiotakos DB, Haro JM, Kassebaum NJ, Chrepa V, *et al.* Population prevalence of edentulism and its association with depression and self-rated health. *Sci Rep* 2016;6:37083.
- Kim YK, Ku JK. Guided bone regeneration. *J Korean Assoc Oral Maxillofac Surg* 2020;46:361-6.
- Clementini M, Morlupi A, Canullo L, Agrestini C, Barlattani A. Success rate of dental implants inserted in horizontal and vertical guided bone regenerated areas: A systematic review. *Int J Oral Maxillofac Surg* 2012;41:847-52.
- Titsinides S, Agrogiannis G, Karatzas T. Bone grafting materials in dentoalveolar reconstruction: A comprehensive review. *Jpn Dent Sci Rev* 2019;55:26-32.
- Jensen AT, Jensen SS, Worsaae N. Complications related to bone augmentation procedures of localized defects in the alveolar ridge. A retrospective clinical study. *Oral Maxillofac Surg* 2016;20:115-22.
- Sheikh Z, Hamdan N, Ikeda Y, Grynypas M, Ganss B, Glogauer M. Natural graft tissues and synthetic biomaterials for periodontal and alveolar bone reconstructive applications: A review. *Biomater Res* 2017;21:9.
- Wang HL, Boyapati L. "PASS" principles for predictable bone regeneration. *Implant Dent* 2006;15:8-17.
- Liang Y, Luan X, Liu X. Recent advances in periodontal regeneration: A biomaterial perspective. *Bioact Mater* 2020;5:297-308.
- Eskan MA, Greenwell H, Hill M, Morton D, Vidal R, Shumway B, *et al.* Platelet-rich plasma-assisted guided bone regeneration for ridge augmentation: A randomized, controlled clinical trial. *J Periodontol* 2014;85:661-8.
- Del Corso M, Vervelle A, Simonpieri A, Jimbo R, Inchingolo F, Sammartino G, *et al.* Current knowledge and perspectives for the use of platelet-rich plasma (PRP) and platelet-rich fibrin (PRF) in oral and maxillofacial surgery part 1: Periodontal and dentoalveolar surgery. *Curr Pharm Biotechnol* 2012;13:1207-30.
- Choukroun J, Adda F, Schoffler C, Vervelle A. The opportunity in perio-implantology: the PRF. *Implantodontie* 2001;42:55-62.
- Zhang Y, Ruan Z, Shen M, Tan L, Huang W, Wang L, *et al.* Clinical effect of platelet-rich fibrin on the preservation of the alveolar ridge following tooth extraction. *Exp Ther Med*

- 2018;15:2277-86.
15. Kumar RV, Shubhashini N. Platelet rich fibrin: A new paradigm in periodontal regeneration. *Cell Tissue Bank* 2013;14:453-63.
 16. Souza Magalhães V, Alves Ribeiro R, Leite Do Amaral JM, Castro Pimentel A, Paulim LA, Roman-Torres CV. The use platelet rich fibrin in dental implants: A literature review. *Trend Transplant* 2018;11:1-3.
 17. Kökdere NN, Baykul T, Findik Y. The use of platelet-rich fibrin (PRF) and PRF-mixed particulated autogenous bone graft in the treatment of bone defects: An experimental and histomorphometrical study. *Dent Res J (Isfahan)* 2015;12: 418-24.
 18. Sohn DS, Huang B, Kim J, Park WE, Park CC. Utilization of autologous concentrated growth factors (CGF) enriched bone graft matrix (Sticky bone) and CGF-enriched fibrin membrane in implant dentistry. *J Implant Adv Clin Dent* 2015;7:11-8.
 19. Percie Du Sert N, Hurst V, Ahluwalia A, Alam S, Avey MT, Baker M, *et al.* The ARRIVE guidelines 2.0: Updated guidelines for reporting animal research. *PLoS Biol* 2020;18:e3000410.
 20. Wu T, Jin Y, Ni Y, Zhang D, Kato H, Fu Z. Effects of light cues on re-entrainment of the food-dominated peripheral clocks in mammals. *Gene* 2008;419:27-34.
 21. Wu T, Ni Y, Dong Y, Xu J, Song X, Kato H, *et al.* Regulation of circadian gene expression in the kidney by light and food cues in rats. *Am J Physiol Regul Integr Comp Physiol* 2010;298:R635-41.
 22. Xu L, Wu T, Li H, Ni Y, Fu Z. An individual 12-h shift of the light-dark cycle alters the pancreatic and duodenal circadian rhythm and digestive function. *Acta Biochim Biophys Sin (Shanghai)* 2017;49:954-61.
 23. Garber J, Barbee W, Bielitzki J, Clayton L, Donovan J, Kohn D, *et al.* *Guide for the Care and Use of Laboratory Animals*. Washington, D.C.: National Academies Press; 2011.
 24. Fujioka-Kobayashi M, Miron RJ, Hernandez M, Kandalam U, Zhang Y, Choukroun J. Optimized platelet-rich fibrin with the low-speed concept: Growth factor release, biocompatibility, and cellular response. *J Periodontol* 2017;88:112-21.
 25. Diehl KH, Hull R, Morton D, Pfister R, Rabemampianina Y, Smith D, *et al.* A good practice guide to the administration of substances and removal of blood, including routes and volumes. *J Appl Toxicol* 2001;21:15-23.
 26. Mourão CF, Lowenstein A, Mello-Machado RC, Ghanaati S, Pinto N, Kawase T, *et al.* Standardization of animal models and techniques for platelet-rich fibrin production: A narrative review and guideline. *Bioeng (Basel)* 2023;10:482.
 27. Herrera-Vizcaino C. Systematic review of platelet-rich fibrin (PRF) centrifugation protocols in oral and maxillofacial surgery and the introduction of AR2T3: An easy to remember acronym to correctly report vertical and horizontal PRF centrifugation. *Front Oral Maxillofac Med* 2023;5:2-20.
 28. Oh SS, Narver HL. Mouse and rat anesthesia and analgesia. *Curr Protoc* 2024;4:e995.
 29. Hasuie A, Ujiie H, Senoo M, Furuhashi M, Kishida M, Akutagawa H, *et al.* Pedicle periosteum as a barrier for guided bone regeneration in the rabbit frontal bone. *In vivo* 2019;33:717-22.
 30. Bosch C, Melsen B, Vargervik K. Importance of the critical-size bone defect in testing bone-regenerating materials. *J Craniofac Surg* 1998;9:310-6.
 31. Leary SL, Underwood W, Anthony R, Cartner S, Grandin T, Greenacre C, *et al.* *AVMA guidelines for the euthanasia of animals: 2020 edition*. United States: American Veterinary Medical Association; 2020.
 32. Vajgel A, Mardas N, Farias BC, Petrie A, Cimões R, Donos N. A systematic review on the critical size defect model. *Clin Oral Implants Res* 2014;25:879-93.
 33. Tadjoeidin ES, De Lange GL, Bronckers AL, Lyaruu DM, Burger EH. Deproteinized cancellous bovine bone (Bio-Oss ®) as bone substitute for sinus floor elevation. *J Clin Periodontol* 2003;30:261-70.
 34. Park JY, Hong KJ, Ko KA, Cha JK, Gruber R, Lee JS. Platelet-rich fibrin combined with a particulate bone substitute versus guided bone regeneration in the damaged extraction socket: An *in vivo* study. *J Clin Periodontol* 2023;50:358-67.
 35. He L, Lin Y, Hu X, Zhang Y, Wu H. A comparative study of platelet-rich fibrin (PRF) and platelet-rich plasma (PRP) on the effect of proliferation and differentiation of rat osteoblasts *in vitro*. *Oral Surg Oral Med Oral Pathol Oral Radiol Endod* 2009;108:707-13.
 36. Clark D, Rajendran Y, Paydar S, Ho S, Cox D, Ryder M, *et al.* Advanced platelet-rich fibrin and freeze-dried bone allograft for ridge preservation: A randomized controlled clinical trial. *J Periodontol* 2018;89:379-87.